THE JOURNAL OF PHYSICAL CHEMISTRY B

Article

pubs.acs.org/JPCB

Calculation of Infrared/Raman Spectra and Dielectric Properties of Various Crystalline Poly(lactic acid)s by Density Functional Perturbation Theory (DFPT) Method

Tingting Lin,[†,‡] Xiang-Yang Liu,[‡] and Chaobin He*[,†,§]

[†]Institute of Materials Research and Engineering, A*STAR (Agency for Science, Technology and Research), 3 Research Link, Singapore 117602

[‡]Department of Physics, National University of Singapore, 2 Science Drive 3, Singapore 117542

[§]Department of Materials Science and Engineering, National University of Singapore, Singapore 117576

Supporting Information

ABSTRACT: We calculated infrared (IR) and Raman spectra of poly(lactic acid) (PLA) polymorphs by employing density functional perturbation theory (DFPT) and a plane wave basis set. Significant different characteristics are found in the calculated spectra of poly(L-lactic acid) (PLLA) α-form and PLLA/poly(D-lactic acid) (PDLA) stereocomplex (sc) form. Particularly in the carbonyl stretching region, there is only one sharp peak in the sc-form while there are five peaks in the PLLA α-form. A low wavenumber (65 cm^{-1}) vibration band of α-PLLA observed in a previous terahertz time-domain spectroscopy study was reproduced in the calculated solid-state PLLA spectra. This band could not be obtained by using DFT (B3LYP/6-31G*) simulation on a single PLA oligomer chain and had been attributed to lattice vibrations in the crystal. The permittivity and polarizability tensors of PLA single crystals were also obtained using the DFPT method and were found to be anisotropic.

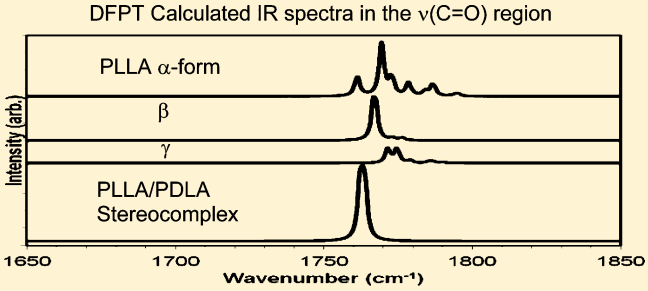

1. INTRODUCTION

Vibrational (Fourier transform infrared (FTIR), Raman, and terahertz (THz)) spectroscopies, being sensitive to the local molecular environment, are some of the important tools for characterization of the chemical and physical natures of polymers. These experimental techniques have been extensively employed to investigate polylactide or poly(lactic acid) (PLA) configuration, conformation, and crystal structures[1,2] and crystallization kinetics (two-dimensional FTIR).[3,4] Early studies mainly focused on the identification of characteristic bands. Cassanas and co-workers first reported a series of vibrational studies on lactic acid,[5] lactides,[6] oligomers,[7] and polymers.[1,2] They found that the C═O stretching mode ν(C═O) of the COOH group was at 1725 cm^{-1} as a strong absorption band in the IR and Raman spectra of lactic acid in aqueous solution.[5] In the solid states of lactides, the ν(C═O) mode of carbonyl groups was a wide band centered at 1763 cm^{-1} in the IR spectrum and three splitting lines at 1758, 1770, and 1779 cm^{-1} in the Raman spectrum.[6] Similar ν(C═O) band splittings at 1750, 1763, and 1774 cm^{-1} were also found in Raman spectra of powdered lactic acid oligomers and polymers.[7] The triplet was attributed to the PLA crystalline region and was speculated to be the result of polymer helical symmetry. The vibration bands were assigned based on molecular symmetry analysis on isolated well-defined PLA helices: a 10_3 helix for crystalline PLLA and a 3_1 helix for 50/50 poly(D-lactic acid) (PDLA)/poly(L-lactic acid) (PLLA) stereocomplex and their analogous correlations to poly(L-alanine) α-helix and poly(propylene) 3_1 helix.[1,2] Although the empirical interpretation on the spectra was straightforward, band assignments were done qualitatively only (i.e., the band wavenumbers were assigned, but the absolute/relative intensities of the bands were unknown). Moreover, crystal packing and the intermolecular interactions in the crystals were ignored because of the assumption of a rigid perfect helix. Hsu and collaborators conducted further spectroscopic analysis on the PLA structure using the normal-coordinate-analysis method by employing a computer program with an adapted force field.[8] This semi-empirical method was capable of giving not only band positions but also relative intensities of the bands. However, the agreement between the calculated and the experimental spectra depends on a number of adjustable input empirical parameters (bond lengths, force constants) and thus depends on the reliability and transferability of the force field implemented. While all the above single-chain approximation vibration analysis results supported X-ray diffraction findings that PLA polymer chains took helical conformations in the crystalline regions, some vibration features remain unexplained. For example, the splitting of the carbonyl stretching (from 1700 to 1850 cm^{-1}) in crystalline

Received: October 21, 2011
Revised: January 8, 2012
Published: January 9, 2012

PLLA and the band shifts of C−H and C═O stretching during the crystallization cannot be explained by the PLA helical structure alone.

Improvements have been made by taking into account crystal space group symmetry and polymer chain intra- and intermolecular interactions (hydrogen bonding and dipole−dipole interactions) in recent studies.[9−12] Hsu et al. included dipole−dipole interactions between the carbonyl C═O groups based on an ab initio calculation on a finite model compound: 2-methoxylpropanoate. They attributed the band splitting in the carbonyl stretch region to the crystal field splitting affected by the carbonyl dipole−dipole interactions.[11] Sarasua and co-workers[9] explained the C−H band shifts in terms of $CH_3\cdots O{=}C$ and $C^{\alpha}H\cdots O{=}C$ hydrogen bonding. The C═O band splitting of low molecular weight PLA caused by intramolecular carbonyl−carbonyl mechanical couplings was qualitatively interpreted using the simply coupled oscillator (SCO) model. They suggested that, to account for the enhanced splitting caused by the electronic effect (Popov et al.), ab initio calculations are required. They attributed the strong split of the E_1 mode centered at about 1759 cm^{-1} to the transition dipole coupling (TDC) interactions and suggested that the excitonic interaction might occur in a collective mode.[12] However, in all these models, long-range electrostatic effects in the crystal and the lattice dynamics had not been considered. The classical dipole−dipole interaction model they adopted is incapable of simulating the interaction involving the dynamic couplings with electron transitions. Therefore, it is necessary to employ a higher level of theory: quantum mechanics and lattice dynamics to account for the electron transition, the long-range electrostatic effects, and collective and lattice vibrations.

Quantum mechanical methods (ab initio or density functional theory (DFT)) have been used to calculate the vibrational spectra of lactic acid,[13] lactides,[14] and PLA oligomers[15] isolated molecules. In our previous studies,[16,17] DFT methods have been utilized to investigate the equilibrium geometries and relative stabilities of the four identified crystalline polymorphs of PLA and their intrinsic elastic properties. To our knowledge, there is no quantum mechanical vibrational spectroscopic study on the crystalline lactide and polylactide. Hence, in this study, we further investigate the lattice dynamic and dielectric properties of these crystals by employing density functional perturbation theory (DFPT) (or the linear response) method.[18] From the DFPT calculations, not only the frequencies but also the intensities of the active IR and Raman modes can be obtained. The DFPT method has been proven reliable in predicting vibrational spectra for various molecular crystals such as amino acids,[19] conjugated polymers,[20] and the high explosive pentaerythritol tetranitrate,[21] as well as many inorganic crystals.[22]

The main purpose of this study is to calculate the entire spectra, frequencies, and intensities of IR and Raman modes, plus silent modes of lactide and polylactide single crystals via the DFPT method and to gain a better understanding of the effects of symmetry, molecular packing, and intermolecular interactions on the vibrational spectra. In the following, in section 2 the computation methods and crystalline models are briefly described, in section 3 detailed results and discussions are included, and finally in section 4 the conclusions appear. Because the calculated spectra contain large quantities of normal modes, only the symmetries and characters of selected vibration modes were presented and analyzed.

2. THEORY AND COMPUTATIONAL DETAILS

Density functional perturbation theory (DFPT)[18] is the preferred method of quantum mechanical calculation of lattice dynamics.[23,24] It provides an analytical way of computing the second derivative of the total energy with respect to a given perturbation. Depending on the nature of this perturbation, a number of properties can be calculated. For example, perturbations in ionic positions and in an electric field cause the dynamic matrix/phonons and the dielectric response, respectively. The DFPT formalism uses a variational technique similar to the density functional theory (DFT) itself; hence it is more robust and accurate than the Green's function scheme.[25,26]

In the phonon description of lattice vibrations, it is assumed that the mean equilibrium position of each ion is a Bravais lattice site and the amplitude of atomic displacements is small compared to interatomic distances. This leads to a harmonic approximation. The harmonic vibrational frequencies can be obtained from the matrix of Cartesian second derivatives, also known as the Hessian matrix, of a molecular or periodic system.[27] The mass-weighted Hessian is obtained by dividing Hessian elements by the square roots of the atomic masses. According to the harmonic approximation, the vibrational frequencies are the square root of the eigenvalues of the mass-weighted force constant matrix (or Hessian) and the normal modes are the eigenvectors. The infrared intensities are obtained from atomic polar tensors (APTs), which are conventionally called Born effective charges in solid-state calculations, of all atoms in the system. The APT is a second derivative of the total energy with respect to the Cartesian coordinates and dipole moments. It yields information on the change in dipole moment under atomic displacements. Further, it is a chargelike quantity derived from the dynamics of the system; as such it may prove more useful in assigning charges to atoms in molecules[19] than conventional Mulliken analysis, which is based upon a rather arbitrary partitioning of electronic charge based on atomic orbitals. The intensity of a given mode can be evaluated as a square of all transition moments of this mode and expressed in terms of the Born effective charge matrix and eigenvectors of the mass-weighted Hessian.

A molecule composed of N atoms has $3N$ degrees of freedom. Diagonalizing the mass-weighted Hessian yields $3N$ frequencies. Of these, six are translations and rotations of the molecule itself and the remaining $3N - 6$ correspond to the normal modes of vibration. In a crystal, there are an infinite number of atoms. The infinite Hessian matrix can be Fourier transformed into an infinite set of $3N \times 3N$ matrices due to the periodicity of the Hessian ($H_{i,j} = H_{i+T,j+T}$), where N stands for the number of atoms in the unit cell and T is the lattice translation vector. There are $3N - 3$ normal modes.

The published experimental crystallographic data for racemic lactide;[28] poly(L-lactide), α-,[29] β-,[30] and γ-forms;[31] and the stereocomplex form between enantiomeric polylactides, sc-form[31] (for a summary of these polymer crystals, see Lin et al.[16,17] and references cited therein), were used as initial atomic positions and crystal symmetries. All atom internal coordinates were optimized to minimize the atomic forces to determine the equilibrium geometry consistent with the system symmetry. The optimized structures were then used in the calculation of IR/Raman spectra and dielectric properties. The calculations were performed using the CASTEP[32] program, in which the wave functions and charge density were expanded in a plane wave basis set. Troullier−Martins norm-conserving pseudopotentials[33] were used

dx.doi.org/10.1021/jp210123q | J. Phys. Chem. B 2012, 116, 1524−1535

to represent the interaction of the valence electrons with the nucleus and the core electrons, therefore greatly enhancing the computational efficiency of the approach. For oxygen atoms in these molecular crystals, a harder pseudopotential with a core radius r_c of 1.4 bohr was implemented. Because of the smaller r_c, a large number of plane waves are needed to represent the wave function well. An energy cutoff of 990 eV of the plane wave basis set was used. The exchange and correlation effects were approximated by the generalized gradient approximation (GGA) of Perdew and Wang.[34]

3. RESULTS AND DISCUSSION

3.1. Vibrational Properties. In this section, the calculated IR/Raman spectra of the above-mentioned five crystals are presented. In order to gain a better understanding of the vibrational normal-mode symmetries and characteristics, first a symmetry analysis on crystal unit cells and the constituent molecules or helices at their isolated states were carried out by employing group theory.

Table 1. Summary of Symmetry Analysis for Isolated Lactide Molecule and Helical PLA Polymer Chain

isolated molecule or helical chain	symmetry group	N^a	internal modes;[b] translational and rotational modes[c]
D- or L- lactide	C_2	18	48, Γ_{vib} = 25A + 23B;
			6, $\Gamma_{trans-rot}$ = 2A + 4B
PLLA 3_1 helix	line group $C(2\pi/3)$ isomorphic to C_3	27	77, Γ_{vib} = 25A + 26E;
			4, $\Gamma_{trans-rot}$ = 2A + E
PLLA 10_3 helix	line group $C(6\pi/10)$ isomorphic to C_{10}	90	266, Γ_{vib} = 25A + 27B + 26E_1 + 27(E_2 + E_3 + E_4);
			4, $\Gamma_{trans-rot}$ = 2A + E_1

[a]Number of atoms. [b]Molecule, $3N - 6$; helix, $3N - 4$. [c]Molecule, 3; helix, 1.

3.1.1. Symmetry Analysis. A nonlinear molecule with N atoms has $3N - 6$ internal modes and three translational and three rotational modes. Lactic acids are optically active compounds, including L- and D-forms. The cyclic dimers of lactic acids, 3,6-dimethyl-1,4-dioxane-2,5-diones ($C_6H_8O_4$), or dilactides (for simplicity, lactides) have three different diastereoisomers, namely, L-lactide(*S*,*S*), D-lactide(*R*,*R*), and *meso*-lactide(*S*,*R*), due to the presence of two chiral centers in the lactides. The free D- or L-lactide molecules possess C_2 point group symmetry. According to the character table of point group C_2, the irreducible representations for the 48 ($3N - 6$, N = 18 atoms) vibrational modes of the D- or L-lactide are Γ_{vib} = 25A + 23B, where all the A and B modes are infrared and Raman active. The three translational and three rotational modes of the molecule are represented as $\Gamma_{trans-rot}$ = 2A + 4B.

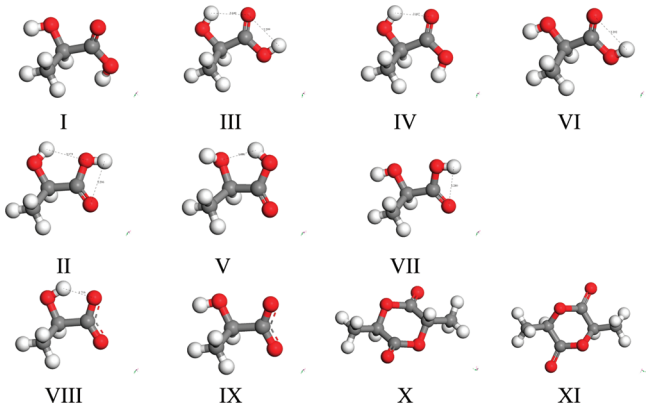

Figure 1. DFT optimized isomer structures of D-lactic acid (I–VII), D-lactate ion (VIII and IX), and lactides (X and XI). The dashed lines indicate the presence of intramolecular hydrogen bonding (HB). The numerical values of the HB distances are included in Table S2 in the Supporting Information.

Table 2. Summary of Symmetry Analysis for the Five Molecular Solids Studied

crystalline unit cell	N;[a] M[b]	space group; site sym (no.); factor group	site sym; no. internal modes (molecule), representations; no. external modes (molecule), representations	factor group sym; no. internal modes (unit cell), representations; no. external modes (unit cell), representations; 3 translational modes of a solid
rac-lactide	72; 4	$P2_1/c$ (C_{2h}^5);	C_i;	C_{2h};
		C_i (4), C_1 (1);	48, Γ_{vib} = 24A_g + 24A_u;	$3N - 6M$ = 192, $\Gamma_{internal}$ = 50A_g + 50A_u + 46B_g + 46B_u;
		C_{2h};	6, $\Gamma_{trans-rot}$ = 3A_u + 3A_g	$6M - 3$ = 21, $\Gamma_{external}$ = 3A_u + 6B_u + 4A_g + 8B_g;
				3, Γ_{trans} = A_u + 2B_u
γ-PLLA	54; 2	$P2_1$ (C_2^2);	C_1;	C_2;
		C_1 (1);	77, Γ_{vib} = 77A;	$3N - 4M$ = 154, $\Gamma_{internal}$ = 77A + 77B;
		C_2;	4, $\Gamma_{trans-rot}$ = 4A;	$4M - 3$ = 5, $\Gamma_{external}$ = 3A + 2B;
				3, Γ_{trans} = A + 2B
β-PLLA	81; 3	$P3_2$ (C_3^3);	C_1;	C_3;
		C_1 (1);	77, Γ_{vib} = 77A;	$3N - 4M$ = 231, $\Gamma_{internal}$ = 75A + 78E;
		C_3	4, $\Gamma_{trans-rot}$ = 4A;	$4M - 3$ = 9, $\Gamma_{external}$ = 5A + 2E;
				3, Γ_{trans} = A + E
α-PLLA	180; 2	$P2_12_12_1$ (C_2^4);	C_1;	D_2;
		C_1 (1);	266, Γ_{vib} = 266A;	$3N - 4M$ = 532, $\Gamma_{internal}$ = 135A + 131B_1 + 133B_2 + 133B_3;
		D_2	4, $\Gamma_{trans-rot}$ = 4A	$4M - 3$ = 5, $\Gamma_{external}$ = 3B_1 + B_2 + B_3;
				3, Γ_{trans} = B_1 + B_2 + B_3
sc-PLA rhombohedral (primitive)	54; 2	$R3c$ (C_{3v}^6);	C_3;	C_{3v};
		C_3 (1), C_1 (1);	77, Γ_{vib} = 25A + 26E;	$3N - 4M$ = 154, $\Gamma_{internal}$ = 25A_1 + 25A_2 + 52E;
		C_{3v}	4, $\Gamma_{trans-rot}$ = 2A + E;	$4M - 3$ = 5, $\Gamma_{external}$ = A_1 + 2A_2 + E;
				3, Γ_{trans} = A_1 + E

[a]Number of atoms. [b]Number of molecules or helices.

dx.doi.org/10.1021/jp210123q | J. Phys. Chem. B 2012, 116, 1524–1535

Table 3. IR C═O Stretching Mode Frequency and Intensity; Intramolecular Hydrogen Bond (HB) Distances for Various Isomers of Lactic Acid, Lactate Ion, and Lactide Calculated Using DMol^3[a]

		IR C═O str freq (cm^{-1})	intensity (km/mol)	equilib C═O bond length (Å)	internal HB $d_{O-H\cdots OH}$ (Å)	internal HB $d_{O-H\cdots O=C}$ (Å)
			D-Lactic Acid, $C_3H_6O_3$			
			In Gas Phase			
III		1755.0 (1778.6)	278.5 (315.0)	1.220 (1.187)		2.049, 2.229 (2.027, 2.289)
			In Water (COSMO)			
V		1740.1	513.4	1.221	1.849	
	expt[b]	1725 (IR/Raman)	strong	ν(C═O)		
			D-Lactate Ion, $C_3H_5O_3$ (Charge $q = -1$)			
			In Gas Phase			
VIII		1673.3 (1679.4)	276.1 (424.6)	1.279, 1.255 (1.243, 1.222)		1.716 (1.734)
	theor[c]	1810 (Raman, SCF), 1662 (Raman, MP_2)				
			In Water (COSMO)			
VIII		1605.0	589.3	1.279, 1.261		1.780
	expt[b]	1585 (IR), 1590 (Raman)	very strong, medium	$\nu_{as}(CO_2^-)$		
			Lactide $C_6H_8O_4$			
			In Gas Phase			
XI		1786.2, 1793.2 (1813.2, 1826.4)	600.4, 34.8 (747.7, 37.8)	1.210, 1.210 (1.176, 1.176)		
	theor[d]	1861.9	563.5	1.204, 1.204		
			In Water (COSMO)			
XI		1738.6, 1754.1	1108, 81.9			
	expt[g]	1745 (Raman), 1720 (Raman)	medium, shoulder	$\nu_{ester\ group}$(C═O), $\nu_{acid\ group}$(C═O)		
			In Solid Phase			
X						
XI		see Table 4		1.187, 1.185		
X	expt[e] (solid)			1.211, 1.187		
XI	expt[f] (solid)			1.200, 1.197		

[a]Values in parentheses are results obtained using CASTEP. [b]Lactic acid 20% aqueous solution, sodium lactate 40% H_2O or D_2O solutions.[5] [c]Gauge invariant atomic orbitals (GIAO).[13] [d]B3LYP/6-31G(d).[14] [e]Reference 38, *meso*-lactide structure. [f]Reference 28, *rac*-lactide structure. [g]Raman L-lactide and D,L-lactide 10% aqueous solution.[6]

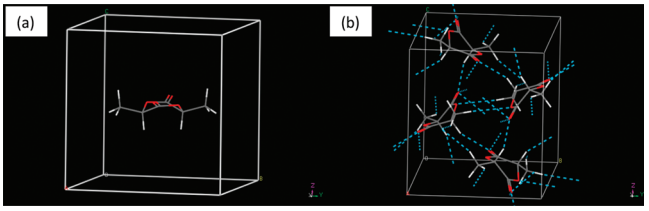

Figure 2. (a) Supercell of an isolated lactide molecule. (b) Intermolecular nonconventional hydrogen bonds (light blue dashed lines) in the racemic lactide crystal.

In the case of a helical polymer chain, there are three translations and one rotation around the helical axis; hence there are $3N - 4$ internal motions. There are nine atoms for each PLA polymer chemical repeat unit ($C_3H_4O_2$). Three such units with a phase angle of 120° form a translational repeat unit of an isolated poly(L-lactide) 3_1 helix. The factor group of the 3_1 helix $C(2\pi/3)$ line group is isomorphic to the point group C_3. The irreducible representations for the 77 ($3N - 4$, where $N = 3{\cdot}9 = 27$) vibrations of the translational repeat unit of PLLA 3_1 helix are $\Gamma_{vib} = 25A + 26E$, where all A and E modes are IR and Raman active, with E modes being doubly degenerate pairs. The three translational and one rotational modes are $\Gamma_{trans-rot} = 2A + E$. Similarly, 10 PLA repeat units with a phase angle of 108° form a translational repeat unit of an isolated poly(L-lactide) 10_3 helical chain. The 10_3 helix belongs to a line group $C(6\pi/10)$ with a factor group which is isomorphic to the cyclic group C_{10}. The irreducible representations of the internal and external modes are shown in Table 1. According to the character table of the group C_{10}, A and E_1 modes are IR and Raman active and E_2 is Raman active only whereas B, E_3, and E_4 modes are inactive.[11]

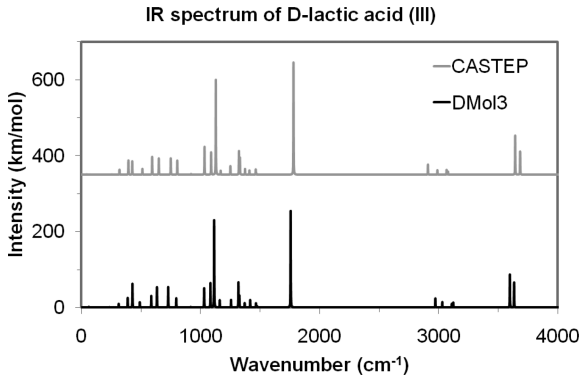

Figure 3. Comparison of IR spectra calculated using DMol^3 (a local basis set and the finite differences method) and CASTEP (a plane wave basis set and the DFPT method) for D-lactic acid molecule (conformation III in Figure 1).

dx.doi.org/10.1021/jp210123q | J. Phys. Chem. B 2012, 116, 1524–1535

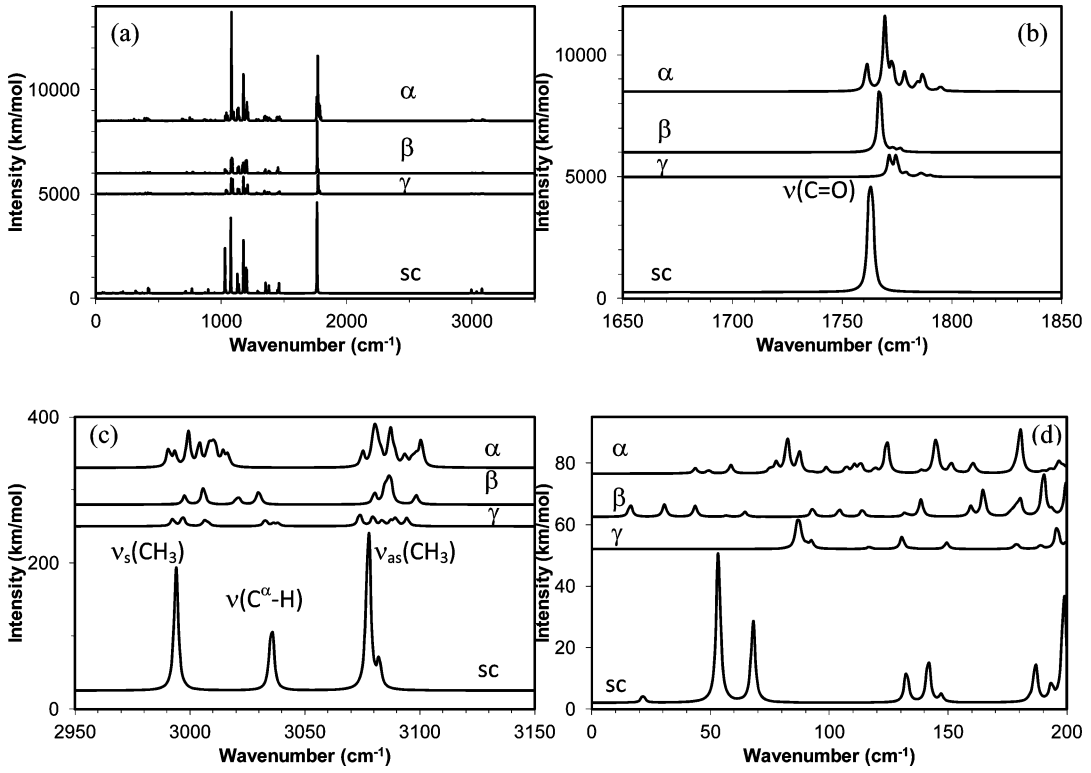

Figure 4. Comparison of the calculated IR spectra of PLLA α-, β-, and γ-forms and PLLA/PDLA stereocomplex (sc), plotted with fwhm = 2 cm^{-1} and graph quality = medium. (a) Full spectra and their expansions in the (b) C=O stretching region, (c) C−H stretching region, and (d) low wavenumbers/THz region. The spectra have been offset in the *y*-axis for clarity.

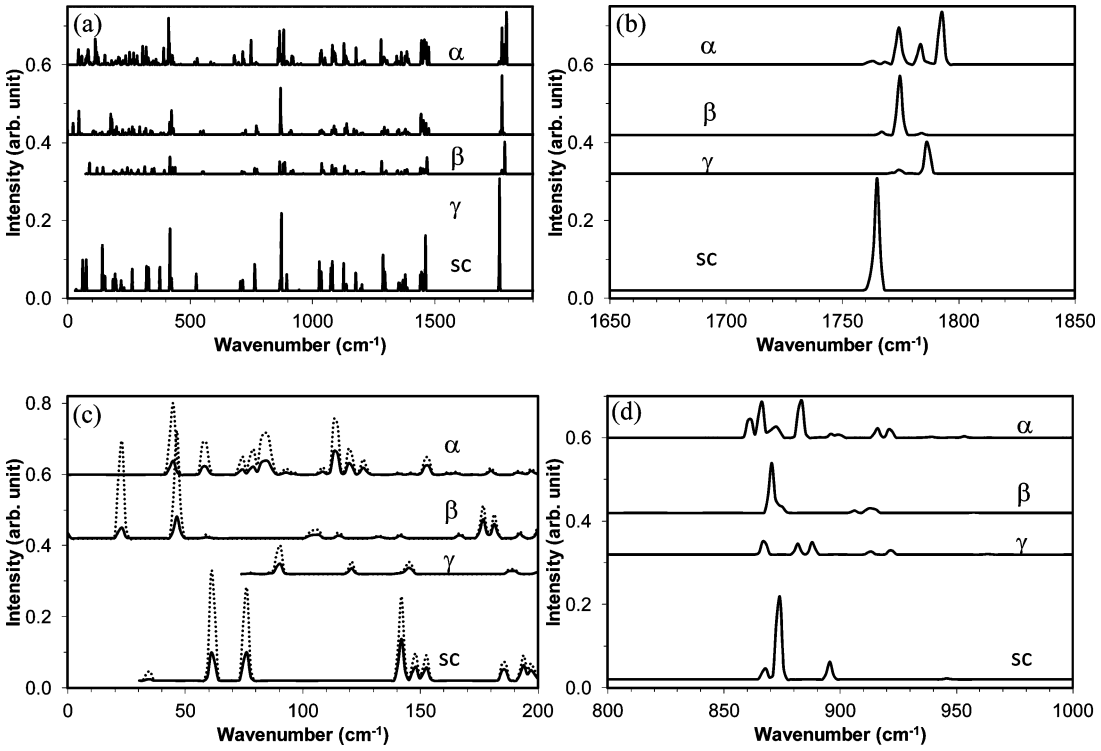

Figure 5. Comparison of the calculated Raman spectra of PLLA α-, β-, and γ-forms and PLLA/PDLA stereocomplex (sc), plotted at T = 10 K and smearing 2 cm^{-1}. (a) Full spectra; (b) 1650−1850 cm^{-1} region; (c) 0−200 cm^{-1} (THz) region, comparison of T = 10 (solid lines) and 300 K (dotted lines); (d) 800−1000 cm^{-1} region. The spectra have been offset in the *y*-axis for clarity.

A crystal unit cell containing M molecules with total N atoms has $3N - 6M$ internal modes, $6M - 3$ external modes (relative rotational and translational motions of the M molecules), and three translational modes of the crystal. Racemic lactide or *rac*-D,L-lactide is an equal molar L-lactide and D-lactide physical mixture. The crystalline structure of racemic lactide was

dx.doi.org/10.1021/jp210123q | J. Phys. Chem. B 2012, 116, 1524−1535

Table 4. Selected Mode Analysis: Transition Frequency, Symmetry/Irrepresentation, IR/Raman Intensities[a]

crystal	freq (cm^{-1})	sym/irr rep	IR int ($(D/Å)^2/amu$)	Raman int ($Å^4$)
racemic lactide		C_{2h}		
	59.3	A_g	0.0	3.41
	60.0	B_g	0.0	1.17
	60.8	B_u	0.27	0.0
	61.9	A_u	0.21	0.0
8 C═O stretching	1761.9	A_g	0.0	153.54
	1766.4	B_g	0.0	10.51
	1769.8	A_u	16.29	0.0
	1774.3	B_u	90.0	0.0
	1780.1	A_g	0.0	498.28
	1786.2	B_u	4.24	0.0
	1788.8	A_u	0.058	0.0
	1793.1	B_g	0.0	24.26
		8 modes	4 IR dark modes, 4 peaks	4 Raman dark modes, 4 peaks
PLLA α-form		D_2		
	43.4	B2	0.04	0.24
	44.8	B1	0.36	1.70
	57.9	A	0.0	1.30
	59.5	B3	0.0038	0.59
	74.2	B1	0.08	1.20
20 C═O stretching	1761.2	B2	26.42	2.48
	1761.4	A	0.0	9.60
	1763.4	B3	0.18	0.81
	1763.6	B1	0.43	12.90
	1768.3	B1	0.05	10.99
	1769.4	B3	70.68	1.36
	1772.8	B2	25.26	1.04
	1774.0	A	0.0	170.22
	1776.1	A	0.0	28.95
	1778.2	B3	1.65	1.54
	1778.4	B2	15.85	0.35
	1780.2	B1	0.75	0.37
	1783.4	A	0.0	94.23
	1784.1	B3	6.81	2.20
	1786.7	B2	15.91	0.81
	1787.1	B1	0.86	9.29
	1792.5	A	0.0	267.29
	1792.6	B3	0.71	1.05
	1794.7	B1	1.88	0.0019
	1795.0	B2	2.59	0.81
		20 modes	5 IR dark modes, 15 peaks	20 peaks
stereocomplex		C_{3v}		
162 atom cell	34.4	A1	0.11	0.16
	48.2	A2	0.0	0.0
	48.7	f	0.0	0.0
	59.8	G	0.0	0.0
	61.5	E	0.26	2.71
	69.0	f	0.0	0.0
	69.5	E	0.62	0.0070
18 C═O stretching	1758.8	e (2-fold)	0.0	0.0
	1762.2	E (2-fold)	38.63	34.16
	1763.6	E (2-fold)	37.22	0.51
	1764.7	A1	0.41	505.07
	1765.7	G (4-fold)	0.0	0.0
	1772.1	G (4-fold)	0.0	0.0
	1774.9	f (2-fold)	0.0	0.0
	1781.2	A2	0.0	0.0
		18 modes	13 dark modes, 5 modes, 3 peaks, 2 of them 2-fold degenerate	13 dark modes, 5 modes, 3 peaks, 2 of them 2-fold degenerate

dx.doi.org/10.1021/jp210123q | J. Phys. Chem. B 2012, 116, 1524−1535

Table 4. continued

crystal	freq (cm^{-1})	sym/irr rep	IR int ($(D/Å)^2/amu$)	Raman int ($Å^4$)
PLLA β-form		C_3		
	22.8	E	0.06	0.36
	46.4	E	0.02	1.38
	48.0	A	0.00056	0.26
	59.2	A	0.05	0.17
9 C=O stretching	1766.9	E	35.22	7.30
	1772.9	E	1.53	0.58
	1774.5	A	0.16	269.5
	1776.2	E	1.70	7.80
	1780.0	A	0.09	0.02
	1784.0	A	0.14	8.67
		9 modes	6 peaks, 3 doubly degenerate E modes	6 peaks, 3 doubly degenerate E modes
PLLA γ-form		C_2		
	77.9	B	0.21	0.12
	86.8	A	0.16	0.26
	89.9	B	0.07	2.55
	90.5	A	0.012	0.043
6 C=O stretching	1771.4	B	19.64	4.95
	1774.5	A	19.53	19.85
	1778.9	B	3.70	2.27
	1785.1	A	2.06	9.31
	1786.5	A	2.49	157.41
	1790.0	B	1.52	0.81
		6 modes	6 peaks	6 peaks

[a]Calculated at the level GGA-PBE/plane wave basis set with energy cutoff 750 eV.

Table 5. Comparison of Born Effective Charges on Hydrogen Atoms H^{α} in Four PLA Crystals[a]

	β-form	γ-form		sc-form		α-form
atom	Z^*_{ave}	Z^*_{ave}	atom	Z^*_{ave}	atom	Z^*_{ave}
$H^{\alpha}(1)$	0.031	0.034	$H^{\alpha}(4)$	0.047	$H^{\alpha}(1)$	0.015
$H^{\alpha}(5)$	0.026	0.031			$H^{\alpha}(5)$	0.003
$H^{\alpha}(9)$	0.020	0.032			$H^{\alpha}(9)$	0.029
					$H^{\alpha}(13)$	0.019
					$H^{\alpha}(17)$	0.010
averaged	*0.026*	*0.032*				*0.015*

[a]PW91/plane wave basis set with cutoff 990 eV.

previously studied by X-ray diffraction, showing that this compound crystallizes in the monoclinic system with a $P2_1/c$ space group and $Z = 4$ molecules (two D- and two L-lactides) in the unit cell. These D- and L-lactides had approximately C_2 symmetry with skew boat conformation.[28] The space group $P2_1/c$ has four sites with symmetry C_i and one site without symmetry C_1. The four molecules were located at the four C_i sites in the unit cell. The symmetry of the site is different from the isolated molecule case (C_2). The representations of modes are summarized in Table 2. The space group $P2_1/c$ is isomorphic to point group C_{2h}. Mapping of the C_i site symmetry onto the factor group C_{2h} gives irreducible representations of the unit cell as shown in the last column of Table 2, where the "g", gerade (even), symmetry modes are Raman active and the "u", ungerade (odd), modes are IR active.

For a crystal unit cell containing M helices with N atoms, there are $3N - 4M$ internal modes, $4M - 3$ external modes, and three translational modes. The space group of PLLA γ-form crystal is $P2_1$ (C_2^2, international number 4). The space group $P2_1$ has one site with symmetry C_1. Two 3_1 helical chains were located at the site with general symmetry C_1 in the unit cell. The factor group of the space group $P2_1$ is point group C_2. Mapping of the C_1 site symmetry onto the factor group gave the irreducible representations as listed in the third row for γ-PLLA in Table 2. Similar analysis was applied to β-PLLA, α-PLLA, and stereocomplex solids. The PLA stereocomplex, which belongs to the trigonal system, may be described by a rhombohedral cell. There are three PLLA and three PDLA 3_1 helices in the conventional hexagonal cell. Each primitive unit cell contains one pair of PLLA and PDLA 3_1 helices. The crystal space group $R3C$ (C_{3v}^6, number 161) is a nonsymmorphic space group. There are six symmetry operations (I $2C_3$ $3\sigma_v$) in the point group of this space group. The set of these point operations forms a group called C_{3v}. The factor group G/T of the space group are isomorphic to C_{3v}. The results are summarized in Table 2. The IR spectra selection rules follow the factor group symmetries of the space groups of these crystals.

3.1.2. Calculated IR/Raman Spectra. The numerical geometry optimization of the five studied crystals of racemic lactide, PLLA α-, β-, γ-forms, and PDLA/PLLA stereocomplex sc-form unit cells were carried out by using density functional theory (DFT) methods at the level of approximations: GGA-PW91-recpot/a plane wave basis set with a cutoff energy of 990 eV. After the optimized structures and the total energies of the ground states were obtained, the dielectric and vibrational properties were further calculated by use of the density functional perturbation theory (DFPT) methods at the same level of approximations unless specified. The results are discussed in the following. The optimized geometric parameters are summarized in Table S1 in the Supporting Information.

The generated IR spectra were smoothed by a Lorentzian function with a full width at half-maximum (fwhm) of 2 cm^{-1} and interpolated onto a grid of about 100 × 100 × 100 (graph quality medium). The frequency of vibration modes was

dx.doi.org/10.1021/jp210123q | J. Phys. Chem. B 2012, 116, 1524–1535

Table 6. Calculated Optical Polarizabilities α_{opt} and Static Polarizabilities α_{dc}

model	Optical polarizability tensor α_{opt} (f -> ∞) (Å^3)	Averaged α_{opt} (Å^3)	Static polarizability tensor α_{DC} (f = 0) (Å^3)	Averaged α_{DC} (Å^3)
L-lactide	$\begin{pmatrix} 15.86 & -1.80 & 0 \\ -1.80 & 14.31 & 0 \\ 0 & 0 & 9.91 \end{pmatrix}$	13.36	$\begin{pmatrix} 18.56 & -2.98 & 0 \\ -2.98 & 16.43 & 0 \\ 0 & 0 & 11.60 \end{pmatrix}$	15.53
D-lactide	$\begin{pmatrix} 15.77 & -1.81 & 0 \\ -1.81 & 14.34 & 0 \\ 0 & 0 & 9.89 \end{pmatrix}$	13.33	$\begin{pmatrix} 18.49 & -2.93 & 0.01 \\ -2.93 & 17.13 & 0.06 \\ 0.01 & 0.06 & 10.61 \end{pmatrix}$	15.41
DL-lactide	$\begin{pmatrix} 15.70 & -1.52 & 0.88 \\ -1.52 & 13.55 & 0.41 \\ 0.88 & 0.41 & 10.53 \end{pmatrix}$	13.26	$\begin{pmatrix} 18.41 & -2.62 & 0.89 \\ -2.62 & 15.50 & 0.34 \\ 0.89 & 0.34 & 14.08 \end{pmatrix}$	16.00
Racemic lactide	$\begin{pmatrix} 80.20 & 0 & -6.31 \\ 0 & 63.86 & 0 \\ -6.31 & 0 & 61.36 \end{pmatrix}$	68.47 (17.12 per molecule)	$\begin{pmatrix} 109.9 & 0 & -7.29 \\ 0 & 84.41 & 0 \\ -7.29 & 0 & 109.4 \end{pmatrix}$	101.3 (25.31 per molecule)
Poly(L-lactide) γ-form	$\begin{pmatrix} 49.02 & 0 & -0.42 \\ 0 & 47.65 & 0 \\ -0.42 & 0 & 54.80 \end{pmatrix}$	50.49 (8.42 per repeat unit)	$\begin{pmatrix} 61.87 & 0 & -1.09 \\ 0 & 57.77 & 0 \\ -1.09 & 0 & 80.06 \end{pmatrix}$	65.57 (10.93 per repeat unit)
Poly(L-lactide) β-form	$\begin{pmatrix} 73.21 & 0 & 0 \\ 0 & 73.21 & 0 \\ 0 & 0 & 81.26 \end{pmatrix}$	75.89 (8.43)	$\begin{pmatrix} 90.42 & 0 & 0 \\ 0 & 90.42 & 0 \\ 0 & 0 & 117.2 \end{pmatrix}$	99.34 (11.04)
Poly(L-lactide) α-form	$\begin{pmatrix} 161.2 & 0 & 0 \\ 0 & 154.9 & 0 \\ 0 & 0 & 178.9 \end{pmatrix}$	165.0 (8.25)	$\begin{pmatrix} 190.1 & 0 & 0 \\ 0 & 186.2 & 0 \\ 0 & 0 & 263.9 \end{pmatrix}$	213.4 (10.67)
Stereocomplex sc-form	$\begin{pmatrix} 49.43 & 0 & 0 \\ 0 & 49.43 & 0 \\ 0 & 0 & 53.40 \end{pmatrix}$	50.75 (8.46)	$\begin{pmatrix} 63.83 & -0.11 & 0 \\ -0.11 & 63.09 & -4.E-5 \\ 0 & -4.E-5 & 83.79 \end{pmatrix}$	70.23 (11.71)

expressed in cm^{-1}, and the intensity was expressed in kilometers per mole. The vertical bars were the normal modes.

3.1.2.1. Single Molecules: Lactic acid, Lactate Ion, and Lactide. To better study the complicated vibrational spectra of PLA crystals, we first presented the calculated spectra for the simple building blocks: lactic acid, lactate ion, and lactide, either in the gas phase (isolated molecules) or in their aqueous solutions. In the present implementation, the PW91 potential, DNP basis set, and fine integration grid of DMol^3 software module[35] were used. The solvent effect was included using the COnductor-like Screening MOdel (COSMO).[36,37]

The chemical structures of lactic acid and lactide molecules are given in Figure S1 in the Supporting Information. The optimized conformations of D-lactic acid, D-lactate ion, and lactides are presented in Figure 1. The calculated results are summarized in Table S2 in the Supporting Information and Table 3. In the gas phase, among D-lactic acid seven (I–VII) possible conformations, III is the most stable one, which has two internal hydrogen bonds (HBs) of type O–H···O═C. In D-lactic acid water solution, however, the most energy favorable conformation is not III but V, which has only one internal HB of type O–H···O–H. Although II has two internal HBs (O–H···O–H and O–H···O═C, respectively), it is less stable than V. When considering the solvent effect, the calculated C═O stretching mode frequency is shifted to a lower wavenumber, 1740 cm^{-1}, compared to that of the gas phase, 1755 cm^{-1}, and is closer to the experimental value of 1725 cm^{-1}.[5] A similar trend applies to the lactate ion. It must be noted that the temperature effect has not been included in our calculations. Because at room temperature kT (T = 25 °C) = 0.592 kcal/mol, as long as the relative energy of an isomer is below 4 kcal/mol ($e^{-\Delta E/kT}$ = 0.1%), such a conformation has a certain population. Actually, the experimental result is a statistical average of a distribution of all possible isomers.

CASTEP calculation of an isolated molecule was carried out using a supercell, i.e., assuming that the molecule is contained within a box (see Figure 2a). Here we used a 10 Å cubic box (the convergence against the box size has been checked; the energy difference is less than 2 meV/atom when the box size is increased up to 15 Å). The calculated results are summarized in Table 3 (values in parentheses). A comparison of the IR spectrum of the D-lactic acid molecule (conformation III) obtained using DMol^3 with that using CASTEP is presented in Figure 3. Overall the two calculated spectra agree well. However, a close examination will find some differences. For example, the C═O stretching mode frequency is at a higher wavenumber, 1778.6 cm^{-1}, using a plane wave basis set and the DFPT method (CASTEP) than the 1755.0 cm^{-1} using an atomic local basis set and finite difference method (DMol^3). For an isolated molecule, employing a local basis set is more

dx.doi.org/10.1021/jp210123q | J. Phys. Chem. B 2012, 116, 1524–1535

convenient and cost-efficient. However, for a molecular crystal, only by employing the DFPT and a plane wave basis set can the IR and Raman intensities be obtained. Hence in the subsequent vibrational spectrum calculations on lactide and polylactide crystals, we used the latter.

3.1.2.2. Lactide and Polylactide Crystals. The calculated IR spectra of PLLA α-, β-, and γ-forms and the stereocomplex sc-form are plotted in Figure 4a with a fwhm = 2 cm^{-1}. In the carbonyl C═O stretching region (Figure 4b), there is only one sharp narrow peak in the stereocomplex while there are five peaks in PLLA α-form and three peaks in PLLA β-form. Moreover, this prominent sc ν(C═O) peak is located at lower wavenumbers when compared to the maximum position of the broad envelope composed of the five peaks of PLLA α-form. This C═O stretching band maximum shift trend agrees well with the early published ambient IR and Raman spectra of PLA 100 and PLA complex.[2] A later cryogenic infrared spectrum of the α-crystal reported by Aou and Hsu has demonstrated the band splitting (1747, 1758, 1762, 1768, and 1777 cm^{-1}) of α-PLLA in this region.[11] Therefore, the DFPT IR spectra agree well with the experimental spectra at very low temperature. Similar band splits were found in the calculated Raman spectra as shown in Figure 5b. The sharper peak of the C═O stretching mode in the sc-form compared to those in other forms is due to the high symmetry restriction. Thirteen of the 18 C═O stretching modes in the sc-form are silent modes, and in the remaining five modes, four modes of are 2-fold degenerate as analyzed and summarized in Table 4. In the C−H stretching region shown in Figure 4c, the locations of three bands, $\nu_s(CH_3)$, $\nu(C^{\alpha}-H)$, and $\nu_{as}(CH_3)$, are very distinguishing in the stereocomplex while those in the α-PLLA are not (where the two $\nu(C^{\alpha}-H)$ and $\nu_s(CH_3)$ bands spread out, overlap, and merge into one wider band). This may be due to the more distorted 10_3 helices in the PLLA α-form. Among the four polymorphs of PLA, only in the sc-form can the helices symmetry (3_1) be kept in the crystal at the site with symmetry C_3. With further analysis on the normal modes, we found that in the sc-form the $\nu(C^{\alpha}-H)$ band moves to a higher wavenumber, even surpassing the $\nu_s(CH_3)$ band. Those in the β- and γ-forms also do so. This reveals that the hydrogen bonding effect on the spectra is larger in the sc-, β-, and γ-forms than in the α-form.

Figures 4d and 5c show the spectra at low wavenumbers which are related to the skeletal rotations and vibrations, and they are sensitive to the temperature as shown in the Raman spectra in Figure 5c. The intensities of these bands increase as the temperature increases from 10 to 300 K. Fuse et al. have reported the observation of two vibration bands of PLLA: 50 and 65 cm^{-1} in the THz region. However, their DFT simulation on a single oligomer chain (up to 28 lactide units) using Gaussian at the level of theory B3LYP/6-31G* could not get the 65 cm^{-1} band and they attributed this band to some lattice vibrations in the crystal and intermolecular interaction. In this study, we are able to simulate these modes by using DFPT at the level of theory GGA-PBE and a plane wave basis set which naturally includes the crystal periodic boundary conditions. As listed in Table 4, in PLLA α-form, these are 43.4 (B2), 44.8 (B1), 59.5 (B3), and 74.2 cm^{-1} (B1). In addition, the B1 modes (parallel to the z axis, i.e., helix axis direction) are relatively stronger than the B2 and B3 modes (perpendicular to the helix axis). In the PLLA β-form, they become 22.8 (E), 44.6 (E, strong), 48.0 (A, weak), and 59.2 cm^{-1} (A, strong), where A modes are parallel to the z axis, i.e., helix axis direction, and E modes are perpendicular to the helix axis. In the stereocomplex, the active modes are 34.4 (A1), 61.5 (E), and 69.5 cm^{-1} (E). Here A1 modes are parallel to the z axis, i.e., helix axis direction, and E modes are perpendicular to the helix axis. Contrary to modes in PLLA α-form, the modes perpendicular to the helix axis are relatively stronger than the modes parallel to the helix axis in the stereocomplex.

An analysis of selected modes for the five studied crystals is given in Table 4. There are four lactide molecules and hence eight carbonyl groups in the racemic lactide crystal unit cell. Only half of the eight C═O stretching modes are IR active due to the factor group symmetry: point group C_{2h}. According to the character table of C_{2h}, the "g", gerade (even), symmetry modes are not IR active. Compared with the isolated lactide molecule (modes 1813.2 and 1826.4 cm^{-1} in Table 3), the C═O stretching mode frequencies of the lactide crystal are shifted to lower wavenumber. There are intermolecular interactions such as nonconventional hydrogen bonds (light blue dashed lines) C−H···O═C and CH_3···−O− in the racemic lactide crystal as shown in Figure 2b.

There are 20 PLA repeat units and therefore 20 carbonyl groups in the PLLA α-form. The factor group of this crystal is the D_2 point group; hence five A modes of the 20 C═O stretching modes are not IR active. Similarly, there are nine and six modes in the β- and γ-forms, respectively. All these modes are IR active. The three E modes in the β-form are doubly degenerate.

The PLA stereocomplex, which belongs to the trigonal system, may be described by a rhombohedral cell. There are three PLLA and three PDLA 3_1 helices in the conventional hexagonal cell. Each primitive unit cell contains one pair of PLLA and PDLA 3_1 helices. The crystal space group $R3C$ (C_{3v}^6, number 161) is a nonsymmorphic space group. There are six symmetry operations (I $2C_3$ $3\sigma_v$) in the point group of this space group. The set of these point operations forms a group called C_{3v}. The factor group G/T of the space group are isomorphic to C_{3v}. In the rhombohedral primitive cell, the six C═O stretching modes are divided into one weak A_1 mode, two strong doubly degenerate E modes, and one A_2 mode which is not IR active, respectively.

3.1.3. Calculated Born Effective Charges. The calculated Born effect charges are presented in Table S3 in the Supporting Information, and a comparison of those on hydrogen atom H^{α} is shown in Table 5. The value of the Born effect charge of the H^{α} hydrogen atom in the stereocomplex is larger than those in other three PLLA forms. This further confirms the strong non-conventional hydrogen bonding (HB) found in the stereocomplex.[16] The Born effect charges may reflect the dynamic characteristics of intermolecular HB interactions better than other static arbitrary portioning of charge methods.[19]

3.2. Polarizability and Permittivity. The calculated dielectric properties are summarized in Tables 6 and 7. The polarizability of lactide in the racemic lactide crystal is larger than those of isolated lactide molecules. This polarizability enhancement may be attributed the change in the molecular electronic structure arising from intermolecular interactions in the crystal. The hydrogen bonds (HBs) are shown in Figure 2b. For each lactide molecule, there are two stronger HBs of $C^{\alpha}-H^{\alpha}\cdots O(=C)$ ($d_{H\cdots O}$ = 2.159 Å, ∠CHO = 157.1°; $d_{H\cdots O}$ = 2.328 Å, ∠CHO = 157.4°) and four weaker HBs of $C^{\beta}-H^{\beta}\cdots O(=C)$ ($d_{H\cdots O}$ = 2.626 Å, ∠CHO = 154.1°; $d_{H\cdots O}$ = 2.662 Å, ∠CHO = 137.7°; $d_{H\cdots O}$ = 2.662 Å, ∠CHO = 136.8°) and of $C^{\beta}-H^{\beta}\cdots-O-$ ($d_{H\cdots O}$ = 2.658 Å, ∠CHO = 172.6°). The C═O bond length of the lactide is about 0.02 Å longer in the crystal

dx.doi.org/10.1021/jp210123q | J. Phys. Chem. B 2012, 116, 1524−1535

Table 7. Calculated Optical Permittivities ε_∞ $(f \to \infty)$and dc Permittivities ε_{dc} $(f \to 0)$[a]

Crystal	Optical permittivity tensor ε_∞ (f -> ∞)	Averaged ε_∞	DC permittivity tensor ε_{DC} (f = 0)	Averaged ε_{DC}
Racemic lactide	$\begin{pmatrix} 2.46 & 0 & -0.12 \\ 0 & 2.16 & 0 \\ -0.12 & 0 & 2.11 \end{pmatrix}$	2.24	$\begin{pmatrix} 2.99 & 0 & -0.13 \\ 0 & 2.53 & 0 \\ -0.13 & 0 & 2.99 \end{pmatrix}$	2.84
Poly(L-lactide) γ-form	$\begin{pmatrix} 2.13 & 0 & -0.01 \\ 0 & 2.09 & 0 \\ -0.01 & 0 & 2.26 \end{pmatrix}$	2.16	$\begin{pmatrix} 2.42 & 0 & -0.03 \\ 0 & 2.33 & 0 \\ -0.03 & 0 & 2.84 \end{pmatrix}$	2.53
Poly(L-lactide) β-form	$\begin{pmatrix} 2.09 & 0 & 0 \\ 0 & 2.09 & 0 \\ 0 & 0 & 2.21 \end{pmatrix}$	2.13	$\begin{pmatrix} 2.35 & 0 & 0 \\ 0 & 2.35 & 0 \\ 0 & 0 & 2.75 \end{pmatrix}$	2.48
Poly(L-lactide) α-form	$\begin{pmatrix} 2.07 & 0 & 0 \\ 0 & 2.03 & 0 \\ 0 & 0 & 2.18 \end{pmatrix}$	2.09	$\begin{pmatrix} 2.26 & 0 & 0 \\ 0 & 2.23 & 0 \\ 0 & 0 & 2.75 \end{pmatrix}$	2.41
Stereocomplex form	$\begin{pmatrix} 2.09 & 0 & 0 \\ 0 & 2.09 & 0 \\ 0 & 0 & 2.18 \end{pmatrix}$	2.12	$\begin{pmatrix} 2.41 & -0.002 & 0 \\ -0.002 & 2.39 & 0 \\ 0 & 0 & 2.85 \end{pmatrix}$	2.55
PLLA Expt.[a]			ε (f = 1 kHz)	2.71

[a]PLLA expt, ref 39.

Table 8. Calculated Intrinsic Principal Refractive Index and the Birefringence

	diagonal ε_∞			principal refractive index			birefringence		
				n_1	n_2	n_3	$\lvert\Delta n_{12}\rvert$	$\lvert\Delta n_{23}\rvert$	$\lvert\Delta n_{13}\rvert$
racemic lactide	2.490	2.159	2.078	1.578	1.469	1.442	0.109	0.027	0.136
poly(L-lactide) γ-form	2.125	2.094	2.259	1.458	1.447	1.503	0.011	0.056	0.045
poly(L-lactide) β-form	2.091	2.091	2.211	1.446	1.446	1.487	0	0.041	0.041
poly(L-lactide) α-form	2.068	2.026	2.185	1.438	1.423	1.478	0.015	0.055	0.040
stereocomplex sc-form	2.090	2.090	2.177	1.446	1.446	1.476	0	0.030	0.030
expt PLLA[a]							0.030−0.033		
α-form[b]							−0.013		

[a]Reference 40. [b]Reference 41, sum of bond polarizability.

(1.198 and 1.199 Å) than that of an isolated molecule, Figure 2a (1.176 Å).

The polarizibility and permittivity tensors of the four polylactide crystals are anisotropic, and some of them are not diagonalized (for the β- and sc-forms the tensors are transversely isotropic due to the crystal symmetries). Among the three diagonalized components of the tensors, the longitudinal component along the polymer helical axis (z axis) is larger than the other two lateral components in the four studied polymer crystals. The averaged values were calculated as one-third of the trace of the tensors (or the arithmetic average of the three principal components).

Because the polylactide crystal unit cells contain various numbers of PLA repeat units, the values of directionally averaged polarizabilities are quite different. These values were further scaled by the PLA repeat unit ($C_3H_4O_2$) numbers containing in the unit cells. A comparison of the four crystals gives, for the static polarizabilities α_{dc} (frequency $f \to 0$), stereocomplex sc-form (11.71) > PLLA β-form (11.04) > PLLA γ-form (10.93) > PLLA α-form (10.67), and the order of optical (frequency $f \to \infty$) polarizabilities is PLLA/PDLA stereocomplex sc-form (8.46) > PLLA β-form (8.43) > PLLA γ-form (8.42) > PLLA α-form (8.25). The specific nonconventional hydrogen bonding network found in the stereocomplex[16] might be responsible for its large dc polarizability enhancement.

The maximum components of the diagonalized dc permittivities ε_{dc} of sc-, γ-, and β-forms were 2.85, 2.84, and 2.75, respectively. The PLA polymer chain took similar 3_1 helical conformations in these three crystals. The only difference is the chain packing pattern. In the sc-form unit cell, the three PLLA left-handed 3_1 helices and three PDLA right-handed 3_1 helices packed in parallel side by side alternatively. In the γ-form the two PLLA left-handed 3_1 helices packed in antiparallel, while in the β-form the three PLLA left-handed 3_1 helices were in parallel. These data indicate that the packing orientation of the helices may have an effect on the permittivity along the chain direction. The antiparallel packing of the same chiral helices or the parallel packing of different chiral helices enhances the permittivity in the chain direction.

The largest component and the average of the three diagonal components of PLLA α-form dc permittivity tensor are 2.75 and 2.41, respectively. The relative permittivity of a PLLA film

dx.doi.org/10.1021/jp210123q | J. Phys. Chem. B 2012, 116, 1524−1535

(thickness 20−250 μm) had been measured at room temperature as a function of frequency in the range 1−10^5 Hz by Ohki and Hirai.[39] Our calculated average dc permittivity is close to but smaller than their experimental result of 2.71 measured at 1 kHz. The published experimental measurement was carried out at ambient temperature and on oriented semicrystalline samples; hence it is an average result of amorphous and polycrystalline samples. To simulate such a system, normally a composite model is required which is beyond the focus of this study. In addition, the experimental samples contained 2−33 wt % additive diethyl hexyl phthalate (DEHP), which may contribute to the polarization. The theoretical calculation is based on a PLA single crystal and calculated at temperature T = 0 K.

From the diagonalized optical permittivities (referring to Table 7), the principal refractive indexes were calculated. Then the differences between these indexes (i.e., the birefringence) were deduced. These data are listed in Table 8 together with published experimental data. The absolute values of the calculated birefringence for the polymer crystals are in the range 0.008−0.056, which encloses the experimental range 0.030−0.033 for PLLA.[40] Kabayashi et al. proposed a different unit cell (two 10_3 helices packed in parallel) for the PLLA α-form and estimated the birefringence value as −0.013 by a summation of bond polarizibility.[41]

4. CONCLUSIONS

In this paper, we have carried out DFPT calculations on the racemic lactide and four polylactide polymorphs systematically. IR and Raman entire spectra and dielectric properties of these single crystals were obtained and compared. The narrow C═O stretching band in the stereocomplex is due to the high symmetry of the crystal which makes most of the modes in this band be IR and Raman inactive. The shift of the $\nu(C^{\alpha}-H)$ band in the stereocomplex to a higher wavenumber may be caused by the intermolecular hydrogen bonding interaction. The earlier experimental observation of low wavenumber vibration bands of α-PLLA, which originate from the collective vibrations of helices in the crystal lattice, was reproduced in our calculations. The simulated spectra in the THz frequency region of the four PLA forms are different. Hence THz spectroscopy could provide an alternative method to differentiate these polymorphs.

■ ASSOCIATED CONTENT

Supporting Information

Structures of L-lactic acid, L-lactide, and a portion of poly(L-lactide) with atomic labels; DFT optimized geometric parameters; relative energies of the various conformations of single molecules; DFPT calculated Born effective charges for the four PLA polymorphs. This material is available free of charge via the Internet at http://pubs.acs.org.

■ AUTHOR INFORMATION

Corresponding Author

*E-mail: cb-he@imre.a-star.edu.sg.

■ REFERENCES

(1) Kister, G.; Cassanas, G.; Vert, M.; Pauvert, B.; Terol, A. *J. Raman Spectrosc.* **1995**, *26*, 307−311.
(2) Kister, G.; Cassanas, G.; Vert, M. *Polymer* **1998**, *39*, 267−273.
(3) Zhang, J.; Tsuji, H.; Noda, I.; Ozaki, Y. *Macromolecules* **2004**, *37*, 6433−6439. Zhang, J.; Tsuji, H.; Noda, I.; Ozaki, Y. *J. Phys. Chem. B* **2004**, *108*, 11514−11520.
(4) Zhang, J.; Sato, H.; Tsuji, H.; Noda, I.; Ozaki, Y. *Macromolecules* **2005**, *38*, 1822−1828. Zhang, J.; Sato, H.; Tsuji, H.; Noda, I.; Ozaki, Y. *J. Mol. Struct.* **2005**, *735*−*736*, 249−257.
(5) Cassanas, G.; Morssli, E.; Fabregue, E.; Bardet, L. *J. Raman Spectrosc.* **1991**, *22*, 409−413.
(6) Kister, G.; Cassanas, G.; Fabregue, E.; Bardet, L. *Eur. Polym. J.* **1992**, *28*, 1273−1277.
(7) Cassanas, G.; Kister, G.; Fabregue, E.; Morssli, E.; Bardet, L. *Spectrochim. Acta, Part A* **1993**, *49*, 271−279.
(8) Kang, S.; Hsu, S. L.; Stidham, H. D.; Smith, P. B.; Leugers, A. M.; Yang, X. *Macromolecules* **2001**, *34*, 4542−4548.
(9) Sarasua, J.-R.; Rodriguez, N. L.; Arraiza, A. L.; Meaurio, E. *Macromolecules* **2005**, *38*, 8362−8371.
(10) Meaurio, E.; Zuza, E.; Lopez-Rodriguez, N.; Sarasua, J. R. *J. Phys. Chem. B* **2006**, *110*, 5790−5800.
(11) Aou, K.; Hsu, S. L. *Macromolecules* **2006**, *39*, 3337−3344.
(12) Meaurio, E.; Martinez de Arenaza, I.; Lizundia, E.; Sarasua, J.-R. *Macromolecules* **2009**, *42*, 5717−5727.
(13) Pecul, M.; Rizzo, A.; Leszczynski, J. *J. Phys. Chem. A* **2002**, *106*, 11008−11016.
(14) Wu, W.; Li, W.; Wang, L.; Zhang, P.; Zhang, J. *J. Mol. Struct.: THEOCHEM* **2007**, *816*, 13−19.
(15) Fuse, N.; Sato, K.; Ohki, Y.; Mizuno, M.; Fukunaga, K. Presented at the 2010 International Conference on Solid Dielectrics, Potsdam, Germany, July 4−9, 2010.
(16) Lin, T. T.; Liu, X. Y.; He, C. B. *Polymer* **2010**, *51*, 2779−2785.
(17) Lin, T. T.; Liu, X. Y.; He, C. B. *J. Phys. Chem. B* **2010**, *114*, 3133−3130.
(18) Baroni, S.; de Gironcoli, S.; Dal Corso, A.; Giannozzi, P. *Rev. Mod. Phys.* **2001**, *73*, 515−562. Refson, K.; Clark, S. J.; Tulip, P. R. *Phys. Rev. B* **2006**, *73*, 155114.
(19) Tulip, P. R.; Clark, S. J. *J. Chem. Phys.* **2004**, *121*, 5201−5210. Tulip, P. R.; Clark, S. J. *Phys. Rev. B* **2006**, *74*, 064301.
(20) Zheng, G.; Clark, S. J.; Tulip, P. R.; Brand, S.; Abram, R. A. *J. Chem. Phys.* **2005**, *123*, 024904. Zheng, G.; Clark, S. J.; Brand, S.; Abram, R. A. *Phys. Rev. B* **2006**, *74*, 165210.
(21) Burnett, A. D.; Kendrick, J.; Cunningham, J. E.; Hargreaves, M. D.; Munshi, T.; Edwards, H. G. M.; Linfield, E. H.; Davies, A. G. *ChemPhysChem* **2010**, *11*, 368−378.
(22) Milman, V.; Refson, K.; Clark, S. J.; Pickard, C. J.; Yates, J. R.; Gao, S.-F.; Hasnip, P. J.; Probert, M. I. J. *J. Mol. Struct.: THEOCHEM* **2010**, *954*, 22−35.
(23) Born, M.; Huang, K. *Dynamical Theory of Crystal Lattices*; Oxford University Press: Oxford, 1954.
(24) Ashcroft, N. W.; Mermin, N. D. *Solid State Physics*; Saunders College: Philadelphia, 1976.
(25) Gonze, X.; Allan, D. C.; Teter, M. P. *Phys. Rev. Lett.* **1992**, *68*, 3603−3606.
(26) Gonze, X. *Phys. Rev. B* **1997**, *55*, 10337−10354.
(27) Wilson, E. B.; Decius, J. C.; Cross, P. C. *Molecular Vibrations*; Dover: New York, 1955.
(28) Van Hummel, G. J.; Harkema, S.; Kohn, F. E.; Feijen, J. *Acta Crystallogr., Sect. B* **1982**, *38*, 1679−1681.
(29) Sasaki, S.; Asakura, T. *Macromolecules* **2003**, *36*, 8385−8390.
(30) Puiggali, J.; Ikada, Y.; Tsuji, H.; Cartier, L.; Okihara, T.; Lotz, B. *Polymer* **2000**, *41*, 8921−8930.
(31) Cartier, L.; Okihara, T.; Ikada, Y.; Tsuji, H.; Puiggali, J.; Lotz, B. *Polymer* **2000**, *41*, 8909−8919.
(32) Clark, S. J.; Segall, M. D.; Pickard, C. J.; Hasnip, P. J.; Probert, M. J.; Refson, K.; Payne, M. C. *Z. Krystallogr.* **2005**, *220* (5−6), 567−570.
(33) Troullier, N.; Martins, J. L. *Phys. Rev. B* **1991**, *43*, 1993−2006.
(34) Perdew, J. P.; Wang, Y. *Phys. Rev. B* **1992**, *45* (23), 13244.
(35) Delley, B. *J. Chem. Phys.* **1990**, *92*, 508. Delley, B. *J. Chem. Phys.* **2000**, *113*, 7756−7764.
(36) Klamt, A.; Schüürmann, G. *J. Chem. Soc., Perkin Trans.* **1993**, *2*, 799. Andzelm, J.; Kölmel, Ch.; Klamt, A. *J. Chem. Phys.* **1995**, *103*, 9312−9320.
(37) Delley, B. *Mol. Simul.* **2006**, *32*, 117−123.

(38) Chisholm, M. H.; Eilerts, N. W.; Huffman, J. C.; Iyer, S. S.; Pacold, M.; Phomphrai, K. *J. Am. Chem. Soc.* **2000**, *122*, 11845−11854.
(39) Ohki, Y.; Hirai, N. *IEEE Trans. Dielectr. Electr. Insul.* **2007**, *14* (6), 1559−1566.
(40) Ohkoshi, Y.; Shirai, H.; Gotoh, Y.; Nagura, M. *Sen'i Gakkaishi* **1999**, *55*, 21−27.
(41) Kobayashi, J.; Asahi, T.; Ichiki, M.; Okikawa, A.; Suzuki, H.; Watanabe, T.; Fukada, E.; Shikinami, Y. *J. Appl. Phys.* **1995**, *77*, 2957−2973.
(42) Brant, D. A.; Tonelli, A. E.; Flory, P. J. *Macromolecules* **1969**, *2*, 228−235.
(43) Okihara, T.; Tsuji, M; Kawaguchi, A.; Katayama, K.; Tsuji, H.; Hyon, S. H.; Ikada, Y. *J. Macromol. Sci., Phys.* **1991**, *B30*, 119−140.